International Journal of Offshore and Coastal Engineering
Vol. 5 | No. 2 | pp. 62-69 | Nov 2021
e-ISSN: 2580-0914

Submitted: July 15, 2021 | Revised: September 17, 2021 | Accepted: October 15, 2021

Fatigue Life Analysis of Mooring System: The Effect of Asymmetry Mooring System Configuration on Single Point Mooring

Revy Maghriza[a*], Eko Budi Djatmiko[a], dan Murdjito[a]

[a)] Departement of Ocean Engineering, Sepuluh Nopember Institute of Technology, Surabaya 60111, Indonesia
**e-mail*: revymaghriza.rm@gmail.com

ABSTRACT

This journal explains the fatigue life analysis of anchor chain in the stand-alone single point mooring by comparing the 4x1 asymmetric and symmetrical mooring system configurations to determine whether the effect of the asymmetrical mooring system configuration on the fatigue life of the anchor chain is related to the length of the mooring lines, the pretensions of the mooring lines, and the angle of spread. The analysis was reviewed on the condition of ULS and FLS environmental loading based on API RP 2 SK code using Orcaflex with 3 hours of time- domain simulation. In the ULS condition, the symmetrical configuration can withstand environmental loads better in the direction of 0° and 180° with the generated maximum tension and maximum offset value smaller than the result from asymmetrical configuration. While the asymmetrical configuration can withstand environmental loads better in the direction of 90° and 270° with the generated maximum tension and maximum offset value smaller than the result from symmetrical configuration. In the FLS condition, the asymmetrical configuration has a longer minimum fatigue life and design life of anchor chain than the symmetrical configuration. This happens because of the spread angle of the mooring line, the length of the mooring line, and the pretension of the mooring line.

Keywords: *Anchor Chain, Tension, T-N Curve, Fatigue Life.*

1. INTRODUCTION

While performing exploration and exploitation activities in the deep sea, floating offshore platforms require a mooring system. One type of mooring system is single point mooring. Single point mooring (SPM) is a permanent mooring system using mooring ropes to tether the shuttle tanker [1]. The mooring system does not completely make the floating structure stationary, but only limits its movement so that it could maintain its position. The movement of floating structures tend to be influenced by environmental loads. Fatigue does not only occur in the structure, but also in the main components and supporting structures. The mooring system is a supporting component of the structure that can fail due to fatigue. Another factor that can affect fatigue life is the asymmetrical mooring scattering angle [2]. In addition, the length of the mooring line also affects fatigue [3, 4]. Therefore, maintenance needs to be done regularly. One form of periodic maintenance is to make modifications by replacing the mooring line. This modification causing the mooring system configuration and the length of mooring line to be less of a concern. Related to the aforementioned problem, fatigue life analysis of the anchor chain will be carried out on SPM which is affected by the asymmetric mooring system configuration. The mooring system configuration that will be used in this analysis is 4x1. Figure 1 shows the top view of mooring system configuration in the SPM and Figure 2 shows the side view of the mooring system configuration to be analyzed:

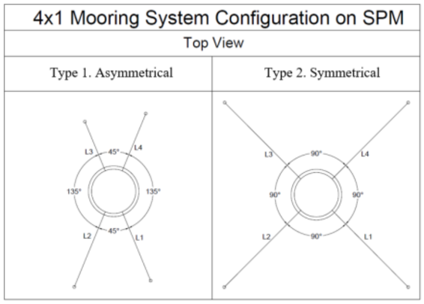

Figure 1. Configuration on The Top View

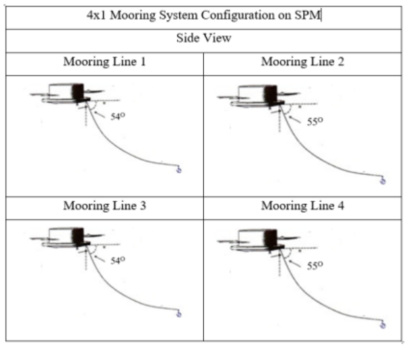

Figure 2. Configuration on The Side View

2. METHODOLOGY

2.1 Collecting Data

The data used in this study were obtained from literature and company studies. SPM data used consist of outer diameter, height, displacement, VCG, etc. Mooring equipment data used are diameter, level, and MBL. While environmental data includes the annual winds, currents, waves, and wave scatter periods of one year.

2.2 Modeling of SPM

SPM modeling is done by using MOSES software. Modeling is done by inputting SPM data that has been obtained previously. Then the modeling results are validated between the hydrostatic results from the moses with the data. The tolerance value of the modeling results on moses and data must be < 2% [5]. The purpose of this tolerance value is to find out whether the modeling resembles its original form or not.

2.3 RAO SPM Analysis on Free Floating Conditions

Motion response analysis of the single point mooring structure is to get the analysis of SPM Response Amplitudo Operator (RAO) on free-floating conditions for every movement, namely translational motion consisting of the surge, sway, and heave and rotations motion consisting of the roll, pitch, and yaw.

2.4 Modeling at Orcaflex

To perform dynamic mooring analysis, SPM and mooring modeling are done on the orcaflex software by inputting the data needed in the orcaflex software.

2.5 Analysis of SPM on Ultimate Limit State Conditions

Tension analysis is carried out at extreme environmental loads (ULS) in intact conditions with a safety factor ≥ 1.67 [6] for mooring tension. In addition, the extreme environmental loads (ULS) is also used for the analysis of the maximum offset on SPM.

2.6 Fatigue Life Analysis of Anchor Chain

Fatigue life analysis of anchor chain with the T-N curve was performed using the rainflow counting method. Then, the annual fatigue damage in each design condition can be obtained which will then be accumulated. The results of this accumulative damage will be used to calculate the fatigue life of the anchor chain. Where the fatigue life must be greater than the design life with a safety factor ≥ 3 for the chain [6].

3. ANALYSIS OF RESULTS AND DISCUSSIONS

3.1 SPM Modeling

SPM modeling was performed using MOSES software with 3D diffraction theory to define the buoy form. Modeling begins by entering the data needed to define the buoy form. The data used in this analysis can be found in Table 1.

Table 1. SPM Data

Description	Symbol	Data	Unit
Displacement	Δ	132.887	ton
Outside Diameter of Buoy	ODB	8.000	m
Outsite Diameter of Skirt	ODS	11.240	m
Height	H	3.700	m
Draft	T	1.800	m
Vertical Center of Gravity	VCG	2.220	m
Radius of Giration	Kxx	2.586	m
	Kyy	2.586	m
	Kzz	3.574	m

The results of SPM modeling on MOSES are in Figure 3 below.

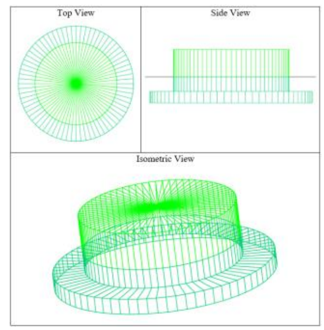

Figure 3. SPM Modeling

3.2 Model Validation

After modeling the MOSES software, the hydrostatic values of the SPM model are validated. The results of the SPM model validation are shown in Table 2.

Table 2. The Results of SPM Validating

Description	Unit	Data	Data	Error
Displacement	ton	132.887	132.887	0.09%
Outside Diameter of Buoy	m	8.000	8.000	0.00%
Outsite Diameter of Skirt	m	11.240	11.240	0.00%
Height	m	3.700	3.700	0.00%
Draft	m	1.800	1.800	0.00%
Vertical Center of Gravity	m	2.220	2.220	0.00%

Based on the validation results above, the hydrostatic properties correction does not exceed 2%, so it can be concluded that the modeling that has been done is feasible to be used in subsequent analysis.

3.3 Motion Response Analysis of SPM on Free Floating Condition

The SPM motion characteristics are presented in RAO graphic form, where the abscissa shows the frequency parameter and the ordinate shows the ratio between the amplitude of the movement in a certain mode [7]. This analysis only evaluates response from 0^0, 45^0, 90^0, 135^0, and 180^0 headings. The RAO graph on SPM free floating conditions is shown in Figure 4-9 below.

a. RAO SPM Analysis of Surge Motion

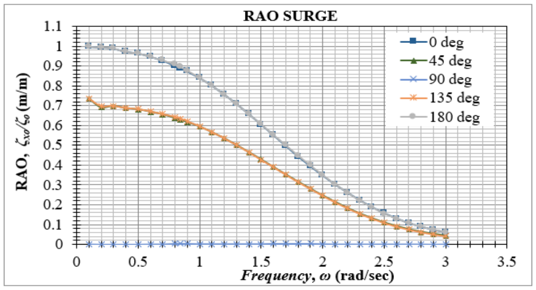

Figure 4. RAO Surge Motion of SPM Free Floating Condition Graph

The largest amplitude occurs at 0° and 180° headings which is 0.997 m/m at 0.1 rad/s wave frequency. Whereas at 90° heading, there is almost no surge movement (0.003 m/m at 0.8 rad/s wave frequency is the largest amplitude).

b. RAO SPM Analysis of Sway Motion

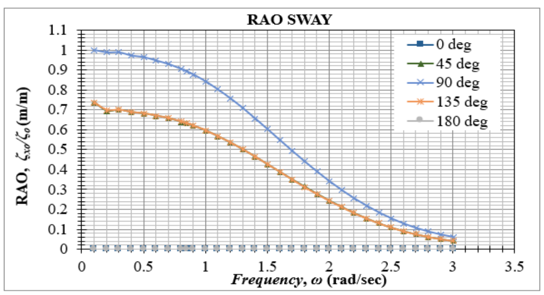

Figure 5. RAO Sway Motion of SPM on Free Floating Condition Graph

The largest amplitude occurs at 90° heading which is equal to 1 m/m at 0.1 rad/s wave frequency. While at 0° and 180° headings, sway do not occur (0.000 m/m at each wave frequency).

c. RAO SPM Analysis of Heave Motion

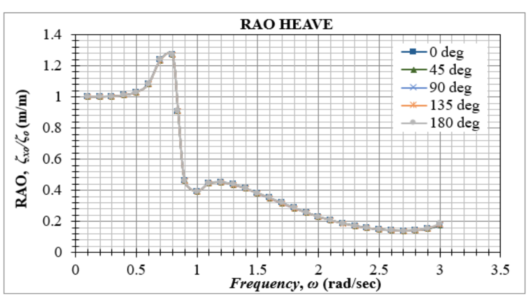

Figure 6. RAO Heave Motion of SPM on Free Floating Condition Graph

Based on the RAO Heave chart above, it can be seen that the same pattern occurs in each heading with the largest amplitude of 1.27 m/m at 0.8 rad/s wave frequency. This is due to the symmetrical shape of the SPM structure.

d. RAO SPM Analysis of Roll Motion

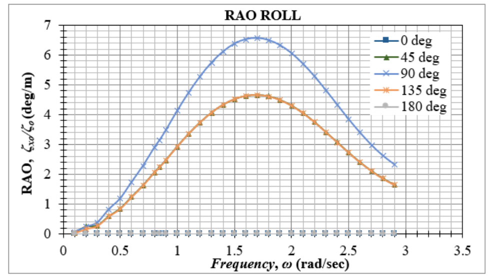

Figure 7. RAO Roll Motion of SPM on Free Floating Condition Graph

The largest amplitude occurs at 90° heading which is 6.57 deg/m with 1.7 rad/s wave frequency. Whereas in the 0° and 180° of headings, there is no roll movement (0.000 deg/m at each wave frequency).

e. RAO SPM Analysis of Pitch Motion

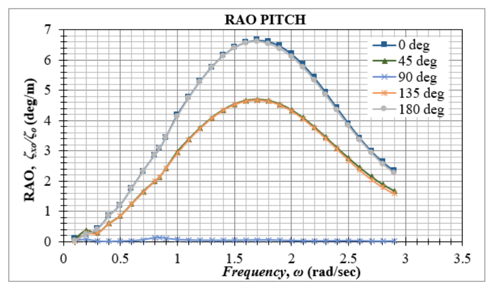

Figure 8. RAO Pitch Motion of SPM on Free Floating Condition Graph

The largest amplitude occurs at 0° and 180° headings which is 6.60 deg/m at 1.7 rad/s wave frequency. Whereas at 90° heading, there is almost no pitch movement (0.119 deg/m at 0.8 rad/s wave frequency is the largest amplitude).

f. RAO SPM Analysis of Yaw Motion

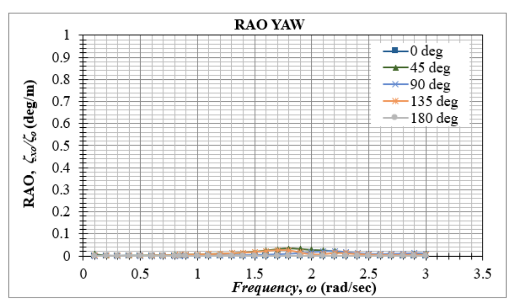

Figure 9. RAO Yaw Motion of SPM on Free Floating Condition Graph

The amplitude of the yaw movement is relatively small. This can be seen from the RAO chart of the yaw movement above. Recapitulation of RAO for each mode of movement of SPM is shown in Table 3.

Table 3. Recapitulation of RAO Comparison for Each Motion in SPM

Mode		Unit	Maxmum RAO					*Maximum Amplitude*
			0°	45°	90°	135°	180°	
Translation	Surge	m/m	1,00	0,74	0,00	0,74	1,00	1,00
	Sway	m/m	0,00	0,74	1,00	0,74	0,00	1,00
	Heave	m/m	1,27	1,27	1,27	1,27	1,27	1,27
Rotation	Roll	deg/m	0,00	4,66	6,57	4,65	0,00	6,57
	Pitch	deg/m	6,65	4,69	0,12	4,67	6,61	6,65
	Yaw	deg/m	0,00	0,03	0,02	0,03	0,00	0,03

3.4 Modeling of Mooring System

The modeling of mooring systems was performed using Orcaflex. The process begins by modeling the single point mooring. Modeling of single point mooring was made by inputting height, diameter, displacement, draft, VCG, the moment of inertia, added mass and damping from MOSES output. SPM modeling in the geometry was modeled as 6D buoy type spar buoy. After modeling the SPM, a mooring line modeling was performed which tethered the SPM to the seabed. The Mooring line property settings are shown in Table 4 and Table 5.

Table 4. Mooring Equipment Data of Asymmetrical Configuration

Description	Unit	Data
Line 1 & 4		
Tipe	-	Studless – Chain
Grade	-	Grade R4
Dimeter	mm	58
Weight in Water	te/m	0.058
Minimum Breaking Load	kN	3627.95
Line 2 & 3		
Tipe	-	Studless – Chain
Grade	-	U3
Dimeter	mm	0.064
Weight in Water	te/m	2600
Minimum Breaking Load	kN	55
Line 2 & 3		
Tipe	-	Studless – Chain
Grade	-	Grade R4
Dimeter	mm	82.5
Weight in Water	te/m	0.118
Minimum Breaking Load	kN	6974.77

Table 5. Mooring Equipment Data of Symmetrical Configuration

Description	Unit	Data
Line 1, 2, 3, & 4		
Tipe	-	Studless – Chain
Grade	-	Grade R4
Dimeter	mm	58
Weight in Water	te/m	0.058
Minimum Breaking Load	kN	3627.95

Then input the coordinates for the two ends of the mooring line in such a way according to the configuration and mooring layout. Mooring layout modeling was done using ORCAFLEX software. Mooring system modeling uses extreme environmental loads (ULS) with 100-year return periods of wind, current, and wave for maximum tension and offset analysis [6]. FLS environmental loading conditions with one year return period from wave scatters for fatigue analysis. The extreme environmental loading conditions (ULS) is inline and between the line. Whereas for FLS environmental loading conditions are inline. The asymmetrical and symmetrical mooring system modeling is shown in Figure 10-13.

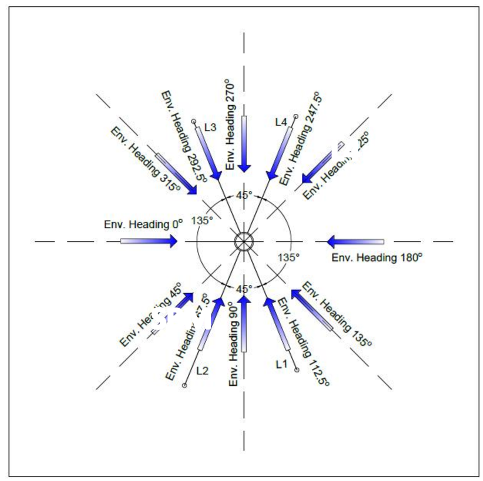

Figure 10. Detail of Asymmetric Mooring System Configuration

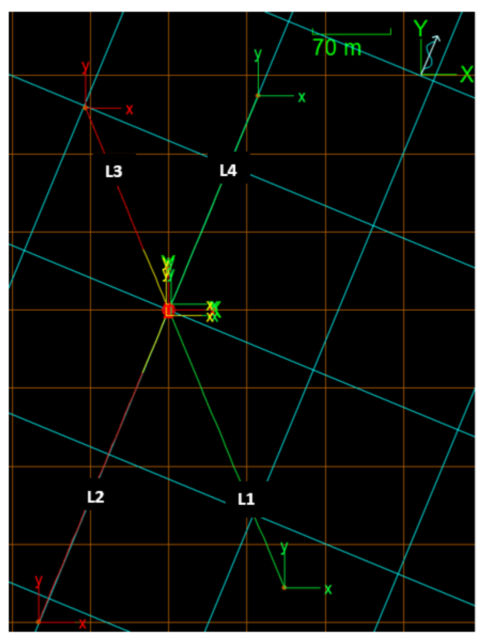

Figure 11. Top view of Asymmetric Mooring System Configuration on in line condition

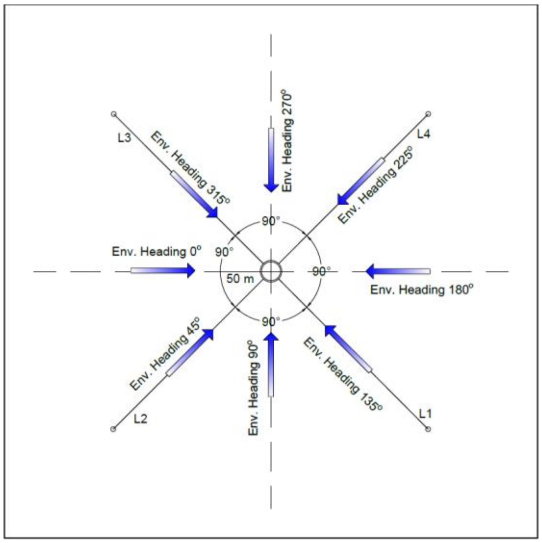

Figure 12. Detail of Symmetric Mooring System Configuration

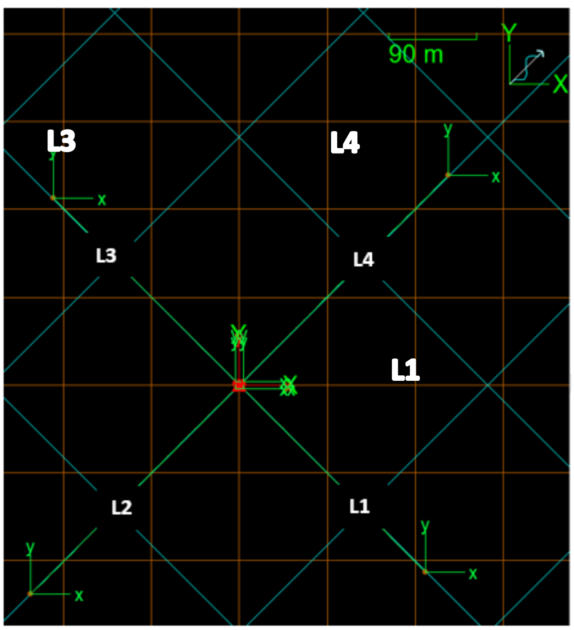

Figure 13. Top view of Symmetric Mooring System Configuration on in line condition

3.5 Maximum Tension Analysis of ULS Conditions

Maximum tension analysis of asymmetrical and symmetrical configuration was performed under intact stability conditions with extreme environmental loading conditions (ULS). The analysis was carried out by simulating time origin of 1800 s. The results of the maximum tension analysis of the two configurations were found in the 0 m segment (End A). The maximum tension results are shown in Figure of graphs 14 and 15.

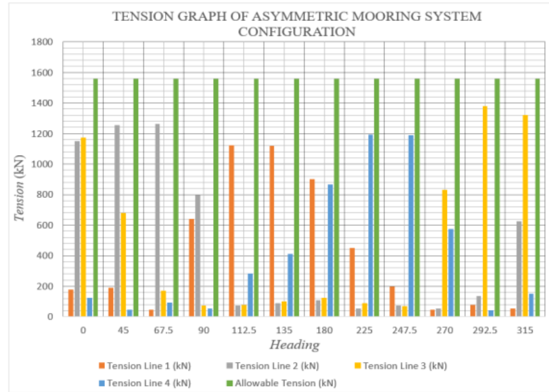

Figure 14. Maximum Tension Graph of Asymmetric Mooring System Configurations

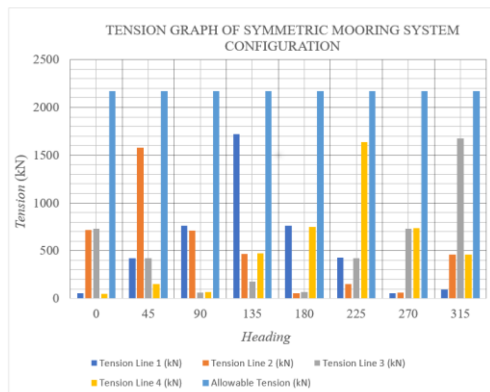

Figure 15. Maximum Tension Graph of Symmetric Mooring System Configurations

3.6 Maximum Offset Analysis of SPM

Dynamic running results on Orcaflex not only produce tension on the mooring line, but also offset on the SPM. The maximum offset in SPM is related to the tension that occurs in the mooring system. The coordinate system and the axis showing the position displacement (offset) on the SPM are shown in Figure 16.

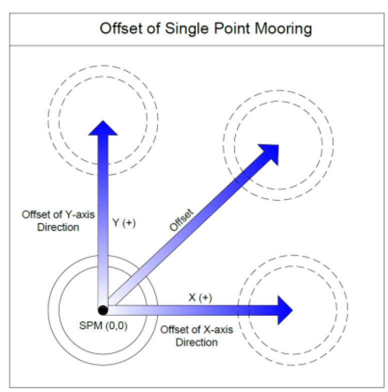

Figure 16. Offset on Single Point Mooring (SPM)

Following are the results of the maximum offset in both configurations shown in graphs 17 and 18.

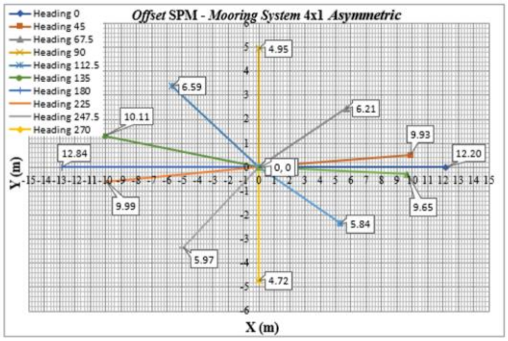

Figure 17. Maximum Offset of SPM on Asymmetric Mooring System Configuration

1

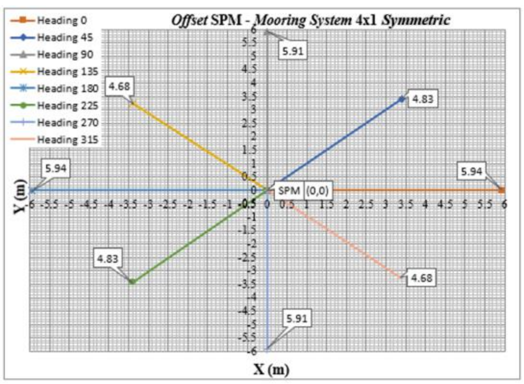

Figure 18. Maximum Offset of SPM on Symmetric Mooring System Configuration

3.7 Fatigue Life Analysis of Anchor Chain

The author simulates the Orcaflex software to obtain the fatigue life of the anchor chain in two configurations. This simulation uses the loading position of the inline environment with the collinear environment loading on the mooring line. Loading simulation for fatigue analysis with 27 sea states based on one year wave scatter is found in table 6.

Table 6. Loading Simulation

Mooring Line	Env. Heading of Asymmetric Configuration	Env. Heading of Symmetric Configuration	Enviromental Load
Line 1	112.5°	135°	27 Seastate
Line 2	67.5°	45°	
Line 3	292.5°	315°	
Line 4	247.5°	225°	

The results of dynamic analysis in the form of tension time history on each sea state are used for fatigue analysis. Examples of tension time history at each anchor chain in the first sea state are shown in figure 19-26.

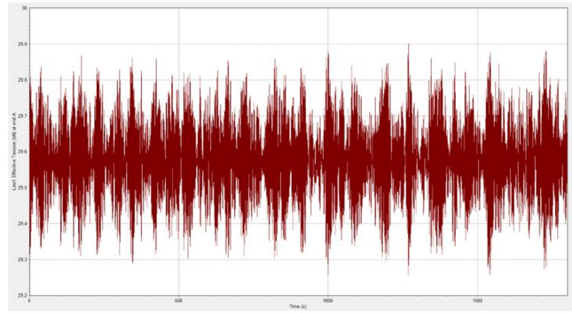

Figure 19. Tension Time History of Anchor Chain 1-Asymmetrical

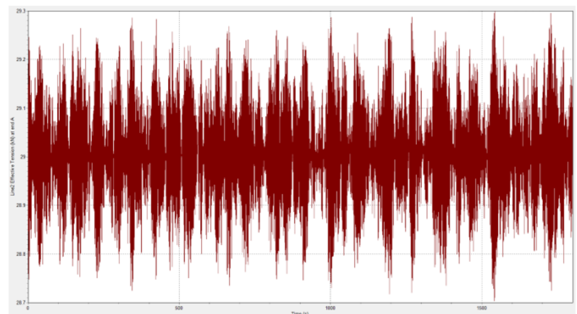

Figure 20. Tension Time History of Anchor Chain 2-Asymmetrical

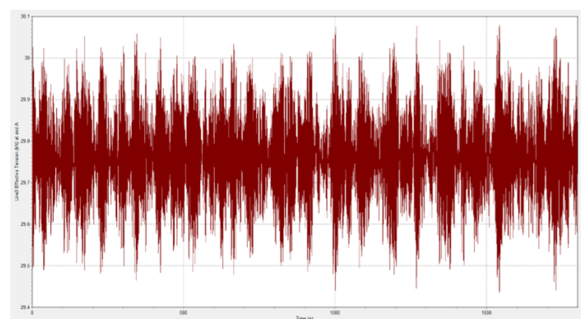

Figure 21. Tension Time History of Anchor Chain 3-Asymmetrical

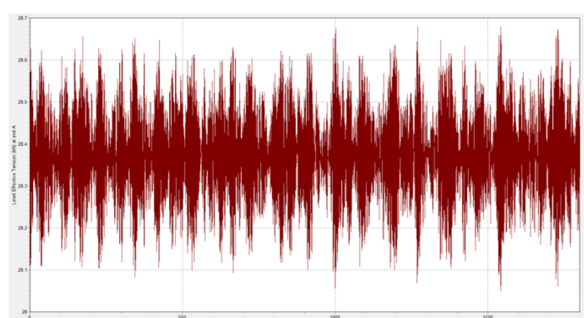

Figure 22. Tension Time History of Anchor Chain 4-Asymmetrical

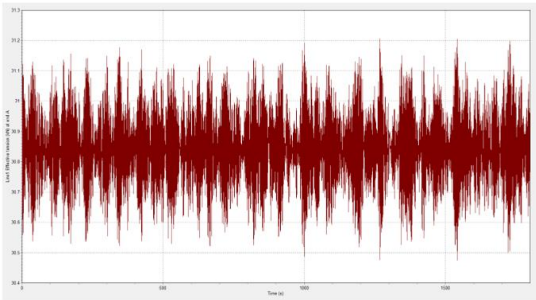

Figure 23. Tension Time History of Anchor Chain 1-Symmetrical

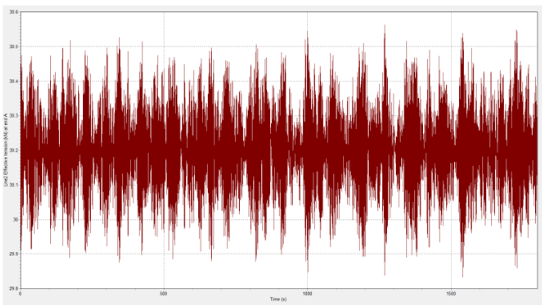

Figure 24. Tension Time History of Anchor Chain 2-Symmetrical

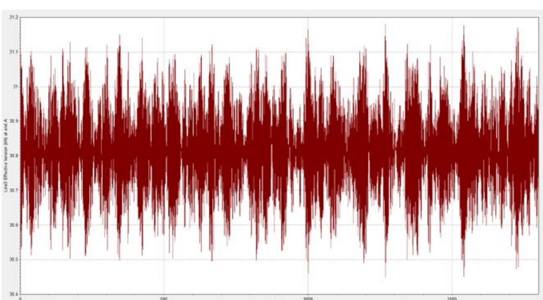

Figure 25. Tension Time History of Anchor Chain 3-Symmetrical

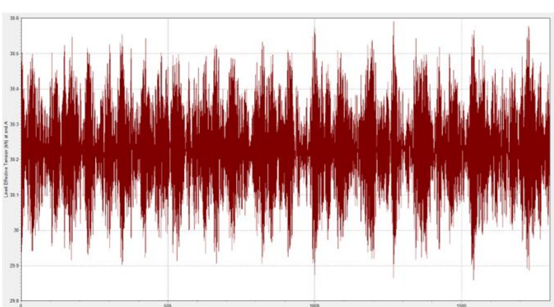

Figure 26. Tension Time History of Anchor Chain 4-Symmetrical

The duration of the fatigue analysis simulation were 1800 s. Based on simulation using T-N curves [8,9] as shown in Figure 27.

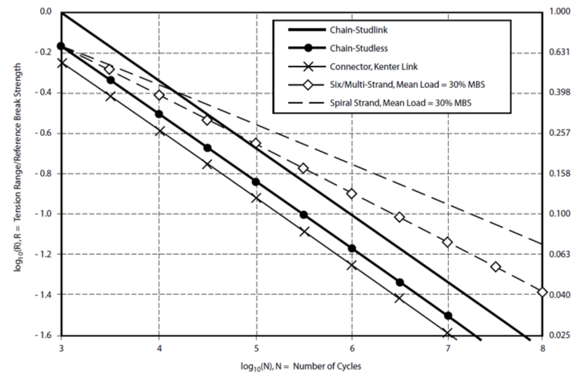

Figure 27. T-N Curve

Then the calculation of the cycle number was performed by the rainflow counting method [10, 11] to get the results of fatigue life on each mooring line for each 4x1 mooring system configuration (asymmetrical and symmetrical). The illustration of the rainflow counting method is shown in Figure 28.

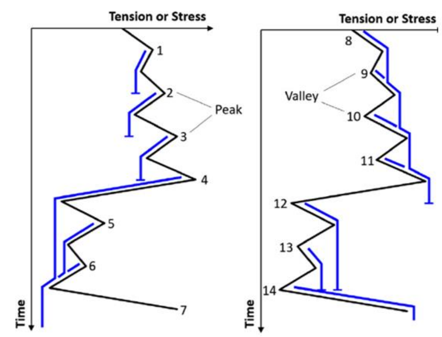

Figure 28. Rainflow Counting Method

Below are the results of anchor chain fatigue life in asymmetrical and symmetrical configurations. Each of the smallest fatigue life on the anchor chain is located in the 0 m segment (end A). Fatigue life results are shown in Tables 7 and 8.

Table 7. The Result of Fatigue Life on Asymmetric Mooring System Configuration

Mooring Line	Property	Declination (°)	Length (m)	Pretension (kN)	Fatigue Life (year)	Design Life (year)
L1	R4 (Dia = 0.058 m)	54	265	13,29	300,16	100,05
L2	R4 (Dia = 0.0825 m) + U3 (Dia = 0.058 m)	55	300	13,48	335,01	111,67
L3	R4 (Dia = 0.0825 m) + U3 (Dia = 0.058 m)	54	195	13,69	306,25	102,08
L4	R4 (Dia = 0.058 m)	55	205	13,01	291,13	97,04

Table 8. The Result of Fatigue Life on Symmetric Mooring System Configuration

Mooring Line	Property	Declination (°)	Length (m)	Pretension (kN)	Fatigue Life (year)	Design Life (year)
L1	R4 (Dia = 0.058 m)	54	270	12,86	208,41	69,47
L2	R4 (Dia = 0.058 m)	55	300	12,52	222,84	74,28
L3	R4 (Dia = 0.058 m)	54	270	12,86	207,57	69,19
L4	R4 (Dia = 0.058 m)	55	300	12,52	223,06	74,35

Based on the table above, it can be seen that the minimum fatigue of asymmetrical anchor chain configuration is longer than the minimum fatigue of symmetrical anchor chain configuration. This happens because of several factors that can be seen in the table, which have been explained in the background, such as the spread angle of the mooring line, the length of the mooring line, and the pretension of the mooring line.

4. CONCLUSIONS

From the results of the analysis conducted by the authors above, the following results are obtained:

1. The symmetrical mooring system configuration is able to withstand environmental loads in the 0° and 180° headings better because the maximum tension result is smaller than the asymmetric mooring system configuration, which is 730.51 kN (Heading 0°) and 762.23 kN (Heading 180°). While the asymmetric mooring system configuration is able to withstand environmental loads in the 90° and 270° headings better because the maximum tension result is smaller than the symmetrical mooring system configuration, which is 53.31 kN (Heading 90°) and 47.87 kN (Heading 270°).
2. The maximum offset result that occurs in SPM also shows that for the symmetrical mooring system configuration is able to withstand the environmental loads in the 0° and 180° headings better because the maximum offset is smaller than the asymmetric mooring system configuration which is equal to 5.94 m. While the asymmetrical mooring system configuration is able to withstand environmental loads in the 90° and 270° headings better because the maximum offset is smaller than the symmetrical mooring system configuration, which is 4.95 m (Heading 90°) and 4.72 m (Heading 270°).
3. The results of fatigue life obtained show that the asymmetric mooring system configuration has a minimum fatigue life of anchor which is longer (291 years with a design life of 97 years) than the symmetrical mooring system configuration (207 years with a design life of 69 years). This happens because of several factors, such as the spread angle of the mooring line, the length of the mooring line, and the pretension of the mooring line.

REFERENCES

1. Chakrabarti, S. K : *Hydrodynamic of Offshore Structure*, Computational Mechanics Publication Shouthampton., Boston, USA, 1987.
2. Shoup, G. J. dan Mueller, R. A.: Failure analysis of a calm buoy anchor system. *Offshore Technology Conference*, Paper No. OTC4764, Cities Service Oil and Gas Corp, 1984.
3. Wu, Y., Wang, T., Eide, Q. dan Haverty, K.: Governing factors and locations of fatigue damage on mooring lines of floating structures, *Research Journal of Ocean Engineering* pp. 109-124, 2015.
4. Prasodjo, B. S., Aristanto, W. D. dan Ashyar, D. F.: Study optimasi panjang mooring line tipe spread mooring pada FPSO, *Research Jurnal of Wave* 5(1), 2011.
5. ABS.: *Dynamic Loading Approach for Floating Production, Storage, and Offloading (FPSO) Installations.*, American Bureau of Shipping, Houston, 2017.
6. API-RP-2SK.: *Recommended Practice for Design and Analysis of Station Keeping System for Floating Structures*. 3rd Ed., API Publishing Services, Washington, DC, 2005.
7. Djatmiko, E. B.: *Perilaku dan Operabilitas Bangunan Laut di Atas Gelombang Acak*., ITS Press, Surabaya, 2012.
8. Ma, K. T., Luo, Y., Kwan, T. dan Wu, Y.: *Mooring System Engineering for Offshore Structur.*, Gulf Professional Publishing, Houston, 2019.
9. Xue, X., Chen , N. Z., Wu, Y., Xiong, Y. dan Gu, Y.: Mooring system fatigue analysis for a semi-submersible, *Research Journal of Ocean Engineering* pp. 550-563, 2018.
10. Olagnon, M. dan Guede, Z.: Rainflow fatigue analysis for loads with multimodal power spectral densities, *Research Journal of Marine Structures* pp. 160-176, 2008.
11. Shafizadeh, E. dan Gharechahi, A.: *A Comparative Study On The Fatigue Life of Mooring Systems for a Wave Dragon (WEC).*, Sharif University of Technology, Tehran, 2015.